

Sparsity Equivalence of Anisotropic Decompositions

Gitta Kutyniok

February 16, 2022

Abstract

Anisotropic decompositions using representation systems such as curvelets, contourlet, or shearlets have recently attracted significantly increased attention due to the fact that they were shown to provide optimally sparse approximations of functions exhibiting singularities on lower dimensional embedded manifolds. The literature now contains various direct proofs of this fact and of related sparse approximation results. However, it seems quite cumbersome to prove such a canon of results for each system separately, while many of the systems exhibit certain similarities.

In this paper, with the introduction of the concept of *sparsity equivalence*, we aim to provide a framework which allows categorization of the ability for sparse approximations of representation systems. This framework, in particular, enables transferring results on sparse approximations from one system to another. We demonstrate this concept for the example of curvelets and shearlets, and discuss how this viewpoint immediately leads to novel results for both systems.

Key Words. Atomic Decompositions. Curvelets. Geometric Separation. Parabolic Scaling. Shearlets. Sparse Approximation.

Acknowledgements. The author would like to thank Peter Binev, Emmanuel Candès, Wolfgang Dahmen, Philipp Grohs, Demetrio Labate, Wang-Q Lim, and Pencho Petrushev for numerous discussions on this and related topics. Special thanks go to David Donoho for enlightening comments and suggestions which helped to improve this work. She would also like to thank the Department of Statistics at Stanford University and the Department of Mathematics at Yale University for their hospitality and support during her visits. This work was partially supported by Deutsche Forschungsgemeinschaft (DFG) Heisenberg fellowship KU 1446/8 as well as DFG Grants KU 1446/13 and KU 1446/14.

1 Introduction

Recently, a paradigm shift could be observed in applied mathematics, computer science, and electrical engineering. The novel paradigm of sparse approximations now enables not only highly efficient encoding of functions and signals, but also provides intriguing new methodologies, for instance, for recovery of missing data or separation of morphologically distinct components. At about the same time, scientists began to question whether wavelets are indeed perfectly suited for image processing tasks, the main reason being that images are governed by edges while wavelets are isotropic objects. This mismatch becomes also evident when recalling that Besov spaces can be characterized by the decay of wavelet coefficient sequences however Besov models are clearly deficient to adequately capturing of edges.

These two fundamental observations have led to the research area of geometric multi-scale analysis whose main goal is to develop representation systems, preferably containing different scales, which are sensitive to anisotropic features in functions/signals and provide sparse approximations of those. Such representation systems shall for now be loosely coined *anisotropic systems*. Let us state as a few samples on the long list the directional filter banks [2], directional wavelets [1], ridgelets [6], complex wavelets [17], (first and second generation) curvelets [9, 10, 11], contourlets [12], bandlets [25], and shearlets [15, 20]. Browsing through the literature, it becomes evident that sparse approximation properties are quite similar for some systems such as curvelets and shearlets, whereas other systems such as ridgelets show a different behavior. Delving more into the literature we observe that for those systems exhibiting similar sparsity behavior many results were proven with quite resembling proofs. One might ask: Is this cumbersome close repetition of proofs really necessary? We believe that the answer is *no* and that a formalization of sparse approximation properties of anisotropic systems solves this problem.

The main goal of this paper is to proclaim the concept of *sparsity equivalence* for anisotropic systems leading to equivalence classes for sparsity properties, and thereby aiming for the aforementioned formalization of sparse approximation properties. Our theoretical considerations are anticipated to have the following impacts:

- A thorough understanding of the ingredients of anisotropic systems which are crucial for an observed sparse approximation property, thereby also categorizing different sparsity behaviors.
- A framework within which sparsity results can be directly transferred from one system to others.
- A quality measure for new anisotropic systems which they have to pass to be considered eligible for a particular sparsity analysis.

1.1 The Concept of Sparsity Equivalence of Frame Expansions

Frame expansions are extensively utilized in applied mathematics, computer science, and electrical engineering if non-uniqueness, yet stability is required, and might be regarded as a natural generalization of the concept of an orthonormal basis. Non-uniqueness of an expansion is customarily exploited for deriving resilience against erasures or quantization. However, lately the flexibility of such non-unique expansions has been shown to lead to

optimally sparse approximations of particular model classes of functions, where sparsity of a coefficient sequence $(c_i)_{i \in I}$ is ideally measured in the $\|\cdot\|_0$ -norm counting the number of non-zero entries. The fundamental fact that this measure can be approximated by the $\|\cdot\|_1$ -norm as the closest convex norm has initiated and led to a deluge of results in the area of sparse approximations and recovery; see the survey paper [4].

Before continuing, let us briefly illustrate the precise relation of this sparsity measure with sparse approximation properties. Given a tight frame $(\varphi_i)_{i \in I}$ for a Hilbert space \mathcal{H} , say, and let $\mathcal{K} \subset \mathcal{H}$ be a class whose elements we desire to sparsely approximate. Approximation theory then paves the way to measure the ability of $(\varphi_i)_{i \in I}$ for sparse approximations of elements of \mathcal{K} , and typically the decay of the squared error of the ‘best’ n -term approximation, i.e., the behavior of

$$\|f - \sum_{n \geq N} (\langle f, \varphi_i \rangle)_{(n)} \varphi_i\|^2 \quad \text{as } N \rightarrow \infty, \quad (1)$$

where $(\langle f, \varphi_i \rangle)_{(n)}$ is the n -th largest coefficient, is analyzed. Intriguingly, in the case of a redundant system, it is not clear whether this is indeed the *best* n -term approximation; nevertheless it is customarily exploited as a suitable substitute in lack of a more accurate and still conveniently applicable selection rule. The term in (1) can now be estimated by

$$\|f - \sum_{n \geq N} (\langle f, \varphi_i \rangle)_{(n)} \varphi_i\|^2 \leq C \cdot \sum_{n \geq N} |(\langle f, \varphi_i \rangle)_{(n)}|^2. \quad (2)$$

Then the relation to $\|(\langle f, \varphi_i \rangle)_i\|_p$ ($0 < p \leq 1$) is established by observing that $\|(\langle f, \varphi_i \rangle)_i\|_p \leq C'$ implies that the number of coefficients $\langle f, \varphi_i \rangle$ exceeding $1/n$ is bounded by $C'n^{1/p}$, thus the magnitude of the n -th largest coefficient $(\langle f, \varphi_i \rangle)_{(n)}$ is not bigger than $C''n^{-1/p}$.

As we already elaborated upon before, there do exist frames which show very similar sparse approximation properties. Aiming towards a categorization of sparsity properties, we immediately observe that the well-exploited unitary equivalence of frames does not serve our purposes here; the reason being that $\|(\langle f, U\varphi_i \rangle)_i\|_p = \|(\langle U^{-1}f, \varphi_i \rangle)_i\|_p$ for all $f \in \mathcal{K}$, however the class \mathcal{K} does not need to be invariant under the unitary operator U^{-1} . Evidently, the equivalence relation we truly aim for is as follows:

Definition 1.1 *Let $(\varphi_i)_{i \in I}$ and $(\psi_j)_{j \in J}$ be two frames for a Hilbert space \mathcal{H} , let \mathcal{K} be a subset of \mathcal{H} , and let $0 < p \leq 1$. Then $(\varphi_i)_{i \in I}$ and $(\psi_j)_{j \in J}$ are sparsity equivalent in ℓ_p with respect to \mathcal{K} , if, for each $f \in \mathcal{K}$, we have $\|(\langle f, \varphi_i \rangle)_i\|_p < \infty$ if and only if $\|(\langle f, \psi_j \rangle)_j\|_p < \infty$.*

This property is in fact a property of the cross-Grammian matrix $(\langle \varphi_i, \psi_j \rangle)_{i,j}$, more precisely, of diagonal dominance of this matrix. A suitable norm for measuring the decay of this matrix away from the diagonal was introduced in [11], and is defined as follows: For $p \in (0, 1]$, the $\|\cdot\|_{O_{p,p}}$ -norm of a matrix $M = (m_{i,j})_{i,j}$ is given by

$$\|M\|_{O_{p,p}} = \max \left\{ \left(\sup_i \sum_j |m_{i,j}|^p \right)^{1/p}, \left(\sup_j \sum_i |m_{i,j}|^p \right)^{1/p} \right\}.$$

This norm indeed measures whether sparsity equivalence is present, and we obtain the following result. Notice however, that the condition on the cross-Grammian matrix is by far not necessary, which can be seen by the fact that it implies sparsity equivalent in ℓ_p with respect to *any* subset \mathcal{K} .

Lemma 1.1 *Let $(\varphi_i)_{i \in I}$ and $(\psi_j)_{j \in J}$ be two tight frames for a Hilbert space \mathcal{H} , let \mathcal{K} be a subset of \mathcal{H} , and let $0 < p \leq 1$. If $\|(\langle \varphi_i, \psi_j \rangle)_{i,j}\|_{O_{p,p}}$ is finite, then $(\varphi_i)_{i \in I}$ and $(\psi_j)_{j \in J}$ are sparsity equivalent in ℓ_p with respect to \mathcal{K} .*

Proof. Let $f \in \mathcal{C}$, and assume that $\|(\langle f, \varphi_i \rangle)_i\|_p < \infty$. From $\|(\langle \varphi_i, \psi_j \rangle)_{i,j}\|_{O_{p,p}} < \infty$ it follows that

$$\sup_i \sum_j |\langle \varphi_i, \psi_j \rangle|^p < \infty \quad \text{and} \quad \sup_j \sum_i |\langle \varphi_i, \psi_j \rangle|^p < \infty. \quad (3)$$

Using the fact that $(\varphi_i)_i$ is a tight frame,

$$\|(\langle f, \psi_j \rangle)_j\|_p^p = \|(\sum_i \langle f, \varphi_i \rangle \varphi_i, \psi_j)_j\|_p^p = \|(\sum_i \langle f, \varphi_i \rangle \langle \varphi_i, \psi_j \rangle)_j\|_p^p.$$

Now, since $p \leq 1$,

$$\|(\sum_i \langle f, \varphi_i \rangle \langle \varphi_i, \psi_j \rangle)_j\|_p^p \leq \sum_j \sum_i |\langle f, \varphi_i \rangle|^p \cdot |\langle \varphi_i, \psi_j \rangle|^p \leq \sum_i |\langle f, \varphi_i \rangle|^p \cdot \sup_i \sum_j |\langle \varphi_i, \psi_j \rangle|^p,$$

which is finite by (3) and due to the fact that $\|(\langle f, \varphi_i \rangle)_i\|_p < \infty$.

For symmetry reasons, the implication $\|(\langle f, \psi_j \rangle)_j\|_p < \infty \Rightarrow \|(\langle f, \varphi_i \rangle)_i\|_p < \infty$ can be derived similarly. The lemma is proved. \square

We will now demonstrate this concept for the pair of curvelets and shearlets, which are two prominent examples of anisotropic systems even sharing parabolic scaling as the main anisotropic force. The intuition that they should be sparsity equivalent is substantiated by comparing results on sparse approximation properties of curvelets and shearlets. And, in fact, the result derived in Subsection 1.3 shows this to be true. Before stating the result, we first need to introduce those two systems.

1.2 Curvelets and Shearlets

We now recall the definitions of curvelets – focussing on second generation curvelets – and shearlets. Those two systems will be exemplarily focused on in our demonstration of the framework of sparsity equivalence.

1.2.1 Curvelets

The main motivation for the introduction of curvelets came from the observation that – by taking a computer vision point of view – edges are those features governing an image while separating smooth regions. A first model for this view point was introduced in [13] and coined a ‘cartoon-like model’. This model then in fact revealed the suboptimal treatment of edges by the at that time seemingly superior system of wavelets.

The introduction of (first generation) tight curvelet frames in 2004 by Candés and Donoho [9], which provably provide (almost) optimally sparse approximations within such a cartoon-like model might be considered a milestone in applied harmonic analysis. Later, second generation curvelets were introduced in [11] due to a more satisfactory associated system with continuous parameters [10], and were shown to provide optimally sparse decompositions of Fourier Integral Operators [5].

To present the definition of these second generation curvelets – from now on also called *curvelets* in contrast to *first generation curvelets* –, let W be the Fourier transform of a one-dimensional wavelet and V be a ‘bump function’ in Fourier space. We select both functions to be band-limited, where $\text{supp } W \subseteq [-2, -1/2] \cup [1/2, 2]$ and $\text{supp } V \subseteq [-1, 1]$, and to satisfy $W, V \in C^\infty$. Curvelets live on anisotropic regions of width 2^{-j} and length $2^{-j/2}$ at various orientations, which are parameterized by angle. For our purposes, it is sufficient to ignore the low frequency part in curvelet decompositions as discussed latter. We just mention that appropriate low frequency functions can be added to the curvelet system defined below to force it to become a tight frame for $L^2(\mathbb{R}^2)$. Hence we will only state the definition of curvelets restricted to

$$\mathcal{C} = \{\xi \in \mathbb{R}^2 : \|\xi\|_\infty \geq 1\}.$$

Let now A_a denote the parabolic scaling matrix $A_a = \text{diag}(a, \sqrt{a})$. *Curvelets* at scale $j \geq 0$, orientation $\ell = 0, \dots, 2^{j/2} - 1$, and spatial position $m = (m_1, m_2) \in \mathbb{Z}^2$ are then defined by their Fourier transforms of some $\xi \in \mathbb{R}^2$, with (r, ω) denoting the associated polar coordinates,

$$\hat{\gamma}_\mu(\xi) = 2^{-j\frac{3}{4}} \cdot W(r/2^j) V((\omega - \theta_{j,\ell})2^{j/2}) \cdot e^{i\langle R_{\theta_{j,\ell}} A_{2^{-j}} m, \xi \rangle},$$

where here $\theta_{j,\ell} = 2\pi\ell/2^{j/2}$, R_θ is planar rotation by $-\theta$ radians, and we let $\mu = (j, \ell, m)$ index scale, orientation, and position. We refer to [11, Sect. 4.3, pp. 210-211] for more details, and to Figure 1 for an illustration of the induced tiling of the frequency plane.

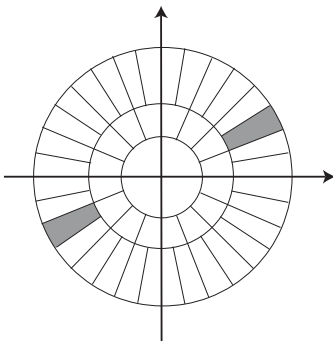


Figure 1: The tiling of the frequency domain induced by curvelets.

1.2.2 Shearlets

In 2006, a novel directional representation system – so-called shearlets – has been proposed in [15, 20], which provides a unified treatment for the continuum and digital world. The main point in comparison with curvelets is the fact that angles are replaced by slopes when parameterizing directions which greatly supports the treating of the digital setting. Hence the theory of shearlets allows an associated digital theory which can be directly implemented [23].

In a similar way as curvelets do shearlets live on anisotropic regions of width 2^{-j} and length $2^{-j/2}$ at various orientations, which are now parameterized by slope rather than angle as for curvelets. Similar to the definition of curvelets stated in Subsection 1.2.1, also here we will ignore the low frequency part, and just mention that it can be appropriately included to yield a tight frame for $L^2(\mathbb{R}^2)$. Let now the Fourier transform W of a wavelet and a bump function V be chosen as in Subsection 1.2.1, and let $\mathcal{C}^{(1)}$ and $\mathcal{C}^{(2)}$ denote the following two cones:

$$\mathcal{C}^{(\iota)} = \begin{cases} \{(\xi_1, \xi_2) \in \mathbb{R}^2 : |\xi_1| \geq 1, |\xi_2/\xi_1| \leq 1\} & : \iota = 1, \\ \{(\xi_1, \xi_2) \in \mathbb{R}^2 : |\xi_2| \geq 1, |\xi_1/\xi_2| \leq 1\} & : \iota = 2. \end{cases}$$

For cone $\mathcal{C}^{(1)}$, at scale $j \geq 0$, orientation $k = -\lceil 2^{j/2} \rceil, \dots, \lceil 2^{j/2} \rceil$, and spatial position $m \in \mathbb{Z}^2$, the associated *shearlets* are defined by their Fourier transforms

$$\hat{\sigma}_\eta(\xi) = 2^{3j/4} \psi(S_k A_{2^j} \cdot -m),$$

where S_k denotes the shear matrix

$$S_k = \begin{pmatrix} 1 & k \\ 0 & 1 \end{pmatrix},$$

and $\eta = (j, k, m, 1)$ indexes scale, orientation, position, and cone. We now assume that $\psi \in L^2(\mathbb{R}^2)$ is chosen such that

$$\hat{\psi}(\xi_1, \xi_2) = W(\xi_1) V(\xi_2/\xi_1),$$

wherefore

$$\hat{\sigma}_\eta(\xi) = 2^{-j\frac{3}{4}} W(\xi_1/2^j) V(k + 2^{j/2} \xi_2/\xi_1) e^{i\langle S_k^T A_{2^{-j}} m, \xi \rangle}.$$

The shearlets for $\mathcal{C}^{(2)}$ are defined likewise by symmetry, as illustrated in Figure 2; this initiated the terminology *cone-adapted shearlets* in contrast to shearlets arising directly from a group representation (cf. [19]).

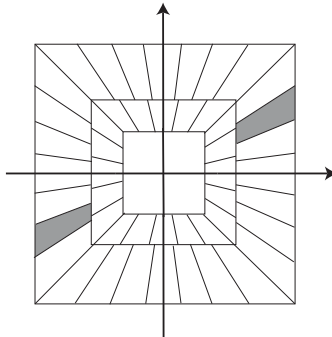


Figure 2: The tiling of the frequency domain induced by cone-adapted shearlets.

We remark that the discrete shearlets considered, for instance, in [16] differ slightly from this choice, since they are usually associated with a scaling of 4^j . However, it is easily

checked – and we refer concerning this issue and additional details to the survey paper [21] – that the shearlets as defined here also form a tight frame for $L^2(\mathbb{R}^2)$.

The attentive reader will have also noticed that we here consider the class of band-limited shearlets although there has just recently been introduced a class of compactly supported shearlets which have superior spatial domain localization (see [22, 18]). Since in this paper we however aim to compare curvelets and shearlets and since curvelets are band-limited, the class of band-limited shearlets is the canonical choice. Another issue to consider is the fact that compactly supported shearlets are not a tight frame, thereby requiring adaptations to the analysis. Additional thoughts on compactly supported versus band-limited shearlets can be found in Section 4.

1.3 Equivalence Result

The introduction of the concept of sparsity equivalence in Subsection 1.1 now motivates us to ask whether curvelets and shearlets belong to the same equivalence class, hence are sparsity equivalent. The many quite similar results on sparse approximation properties of those two systems seem to indicate this. According to Lemma 1.1, the ℓ_p norm of the cross-Grammian matrix reveals the true sparsity relation, and we obtain the following result, whose lengthy proof is presented in Subsection 2.2.

Theorem 1.1 *For all $0 < p \leq 1$,*

$$\|(\langle \sigma_\eta, \gamma_\mu \rangle)_{\eta, \mu}\|_{Op, p} < \infty.$$

Now Lemma 1.1 can be applied to derive the already intuitively expected sparsity equivalence of shearlets and curvelets.

Theorem 1.2 *For all $0 < p \leq 1$, the shearlet frame $(\sigma_\eta)_\eta$ and the curvelet frame $(\gamma_\mu)_\mu$ are sparsity equivalent in ℓ_p with respect to $L^2(\mathbb{R}^2)$.*

1.4 Impact of Sparsity Equivalence

The significance of the viewpoint of sparsity equivalence lies in the fact that it not only provides a thorough understanding of the ability of different anisotropic systems for sparse expansions when compared to each other – thereby providing a qualitative comparison –, but it moreover allows the transfer of sparsity results without repeating quite similar proofs.

The theorem presented in the previous subsection is a first demonstration of the power of such a higher level viewpoint of sparsity behavior. In fact, this result automatically leads to novel results on and insights in sparse expansions by curvelets and shearlets. A few examples, for which this conceptually new approach is fruitful, will be presented in Section 3 including optimally sparse approximations of cartoon-like images and the ability for geometric separation of morphologically distinct phenomena.

1.5 Extensions and General Viewpoint

As mentioned before, Theorems 1.1 and 1.2 are amenable to generalizations and extensions. Previewing Section 4, we briefly discuss a few examples.

- *Curvelets and Shearlets.* A similar statement as Theorem 1.2 should be provable for first generation curvelets as also for the new class of compactly supported shearlets.
- *Other Systems.* The analysis of sparsity equivalence of curvelets and shearlets we drove here can and should be applied to other pairs of systems. Ideally, novelly introduced systems could be compared to a system whose sparse approximation properties are already very well understood.
- *Systems with Continuous Parameters.* Certainly, we can also ask about similar sparsity behavior for systems with continuous parameters. This however requires a different sparsity model; one conceivable path would be to compare their ability to resolve wavefront sets.
- *Weighted Norms.* When aiming at transferring results such as sparse decompositions of curvilinear integrals [7] or sparse decompositions of the Radon transform [8], sometimes weighted ℓ_p norms might need to be analyzed. This is also essential for analyzing associated approximation spaces.

1.6 Outline

We start by presenting the analysis of sparsity equivalence between curvelets and shearlets and providing the proof of Theorem 1.1. We then analyze the impact of this and related results on sparse approximation properties of anisotropic systems in Section 3. In particular, we derive novel results on sparse approximation of cartoon-like images using curvelets and on the ability of geometric separation using shearlets and wavelets. This section is followed by a discussion on extensions of our framework (see Section 4).

2 Sparsity Equivalence between Curvelets and Shearlets

In this section our goal is to prove sparsity equivalence in ℓ_p of curvelets and shearlets for all $0 < p \leq 1$. Due to Lemma 1.1, this task is reduced to proving Theorem 1.1, i.e., showing that the $\|\cdot\|_{O_{p,p}}$ -norm of the cross-Grammian matrix of curvelets and shearlets is finite.

We first realize that for our analysis we only need to consider those curvelets and shearlets which respond to the high-frequency content of a function. More precisely, if we are given a function, say $f \in L^2(\mathbb{R}^2)$, we might decompose it as $f = f_L + f_H = g_L \cdot f + g_H \cdot f$, where g_L is a low pass filter with $(\hat{g}_L)|_{\mathcal{C}} \equiv 1$, and g_H is an ‘associated’ high pass filter satisfying $g_L + g_H = 1$. Now notice, that the inner products between elements of both frames corresponding to g_L are negligible due to their almost orthogonality, since they are scaling functions; also the inner products of those elements with elements corresponding to g_H are of a similar reason negligible.

This argument shows that it is sufficient to only consider the cross-Grammian matrix of the elements of the curvelet and shearlet frame introduced in Subsection 1.2, i.e., those analyzing the high-frequency part of a function.

2.1 Estimates for the Entries of the Cross-Grammian Matrix

We start by establishing estimates on the absolute values of inner products of curvelets and shearlets. An essential ingredient will be the following well-known result, which we state here for the convenience of the reader. A detailed proof might for instance be found in [20, Lem. 2.3].

Lemma 2.1 *Suppose g satisfies $\hat{g} \in C_0^\infty(\mathbb{R}^d)$ with \hat{g} being supported on a fixed bounded rectangle $R \subset \mathbb{R}^d$. Then, for each $N \in \mathbb{N}$, there exists a constant C_N such that*

$$|g(x)| \leq C_N (1 + |x|^2)^{-N} \quad \text{for all } x \in \mathbb{R}^d.$$

In particular, $C_N = N \lambda(R) (\|\hat{g}\|_\infty + \|\Delta^N \hat{g}\|_\infty)$, where $\Delta = \sum_{i=1}^d \frac{\partial^2}{\partial \xi_i^2}$ denotes the frequency domain Laplacian operator and $\lambda(R)$ is the Lebesgue measure of R .

In [11] the following conclusion was drawn from this lemma which we will also require for our proof.

Lemma 2.2 [11, Lem. 5.6] *Suppose $(f_j)_{j \geq 0}$ is a sequence of functions satisfying that each \hat{f}_j is supported in a rectangle $R_j = A_{2^j}([-C_1, C_1] \times [-C_2, C_2])$ and every scaled function*

$$\hat{g}_j(\xi) = 2^{\frac{3}{2}j} \hat{f}_j(A_{2^j} \xi)$$

obeys $\|\hat{g}_j\|_{C^N} \leq \rho_N$ for $N = 2, 4, 6, \dots$ with each ρ_N being independent on j . Then, for $N = 2, 4, 6, \dots$, there exist constants C_N such that

$$|f_j(x)| \leq C_N (\rho_0 + \rho_N) \langle A_{2^j} x \rangle^{-N} \quad \text{for all } x \in \mathbb{R}^d,$$

where

$$\langle y \rangle = (1 + y^2)^{1/2}.$$

The estimates which are proved in the following proposition are carefully designed so that the previously stated claim concerning the $\|\cdot\|_{O_{p,p}}$ -norm, $0 < p \leq 1$ of the cross-Grammian matrix of curvelets and shearlets does follow almost immediately as a corollary. We note that a similar estimate for the second cone $\mathcal{C}^{(2)}$ holds with a resembling proof.

Proposition 2.1 *Let $j, \tilde{j} \geq 0$, $|k| \leq \lceil 2^{j/2} \rceil$, $0 \leq \ell < 2^{j/2}$, and $m, \tilde{m} \in \mathbb{Z}$. Then, for each $N = 2, 4, 6, \dots$, there exist constants C_N so that*

$$|\langle \sigma_{j,k,m,1}, \gamma_{\tilde{j},\ell,\tilde{m}} \rangle| \leq C_N 1_{\{|j-\tilde{j}| \leq 2\}} 1_{\{k \in K_{j,\tilde{j},\ell}\}} 1_{\{\ell \in L_{j,\tilde{j},k}\}} \langle |b_{j,k,m,\tilde{j},\ell,\tilde{m}}| \rangle^{-N}$$

where

$$K_{j,\tilde{j},\ell} = \{k : \lfloor -2^{j/2} \cdot \tan(2^{-\tilde{j}/2}(1 + 2\pi\ell)) - 1 \rfloor \leq k \leq \lceil -2^{j/2} \cdot \tan(2^{-\tilde{j}/2}(-1 + 2\pi\ell)) + 1 \rceil \},$$

$$L_{j,\tilde{j},k} = \{\ell : \lfloor 2^{\tilde{j}/2} \arctan(2^{-j/2}(-1 - k)) - 1 \rfloor \leq 2\pi\ell \leq \lceil 2^{\tilde{j}/2} \arctan(2^{-j/2}(1 - k)) + 1 \rceil \},$$

and

$$b_{j,k,m,\tilde{j},\ell,\tilde{m}} = A_{2^j} (S_k^T A_{2^{-j}} m - R_{\theta_{\tilde{j},\ell}} A_{2^{-\tilde{j}}} \tilde{m}).$$

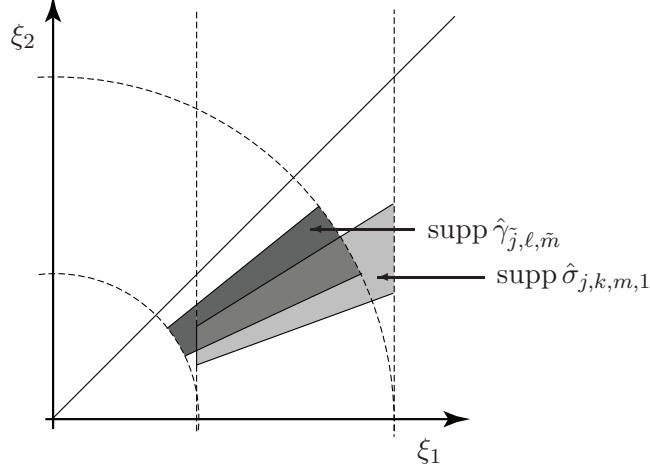


Figure 3: The support in frequency domain of some functions $\sigma_{j,k,m,1}$ and $\gamma_{\tilde{j},\ell,\tilde{m}}$.

Proof. To illustrate the different supports in frequency domain of $\sigma_{j,k,m,1}$ and $\gamma_{\tilde{j},\ell,\tilde{m}}$, a property which will be exploited in the sequel, we refer to Figure 3.

We now fix j, k, m . By employing Plancherel's theorem, we have

$$|\langle \sigma_{j,k,m,1}, \gamma_{\tilde{j},\ell,\tilde{m}} \rangle| = 2^{-(j+\tilde{j})\frac{3}{4}} \int f_{j,\tilde{j},k,\ell}(\xi) \cdot e^{i\langle S_k^T A_{2^{-j}} m - R_{\theta_{\tilde{j},\ell}} A_{2^{-\tilde{j}}} \tilde{m}, \xi \rangle} d\xi, \quad (4)$$

where

$$\hat{f}_{j,\tilde{j},k,\ell}(\xi) = W(\xi_1/2^j)W(r/2^{\tilde{j}})V(k + 2^{j/2}\xi_2/\xi_1)V((\omega - \theta_{\tilde{j},\ell})2^{\tilde{j}/2}).$$

Due to the support conditions of W and V , the support of $\hat{\sigma}_{j,k,m,1}$ equals

$$\text{supp } \hat{\sigma}_{j,k,m,1} = \{(\xi_1, \xi_2) \in \mathbb{R}^2 : \xi_1 \in [2^{j-1}, 2^{j+1}], \xi_2/\xi_1 \in 2^{-j/2}([-1, 1] - k)\}, \quad (5)$$

whereas the support of $\hat{\gamma}_{\tilde{j},\ell,\tilde{m}}$ is

$$\text{supp } \hat{\gamma}_{\tilde{j},\ell,\tilde{m}} = \{(\xi_1, \xi_2) \in \mathbb{R}^2 : r \in [2^{\tilde{j}-1}, 2^{\tilde{j}+1}], \omega \in 2^{-\tilde{j}/2}[-1, 1] + \theta_{\tilde{j},\ell}\}. \quad (6)$$

We conclude that $\hat{f}_{j,\tilde{j},k,\ell} \equiv 0$ unless $|j - \tilde{j}| \leq 2$, hence

$$|\langle \sigma_{j,k,m,1}, \gamma_{\tilde{j},\ell,\tilde{m}} \rangle| \leq C_{j,k,m,\tilde{j},\ell,\tilde{m}} 1_{\{|j-\tilde{j}| \leq 2\}}. \quad (7)$$

Our next task is to estimate the range of ℓ for which $|\langle \sigma_{j,k,m,1}, \gamma_{\tilde{j},\ell,\tilde{m}} \rangle|$ is non-zero. This will be done by showing that this parameter is contained in a compact set whose size is uniformly bounded as $j, \tilde{j} \rightarrow \infty$. For this, we will study the slopes of the boundaries of the supports of $\hat{\sigma}_{j,k,m,1}$ and $\hat{\gamma}_{\tilde{j},\ell,\tilde{m}}$ in angular direction. For better comparison with (5), the support (6) might be rewritten as

$$\text{supp } \hat{\gamma}_{\tilde{j},\ell,\tilde{m}} = \{(\xi_1, \xi_2) \in \mathbb{R}^2 : r \in [2^{\tilde{j}-1}, 2^{\tilde{j}+1}], \xi_2/\xi_1 \in \tan(2^{-\tilde{j}/2}([-1, 1] + 2\pi\ell))\}. \quad (8)$$

Notice that the angle between the two angular boundary lines of the support of curvelets does not change with ℓ , whereas in the shearlet case the angle becomes smaller as the

support of the Fourier transform of the shearlet approaches the angle bisector of the first quadrant. From (5) and (8), it follows that $\hat{f}_{j,\tilde{j},k,\ell} \equiv 0$ if

$$\tan(2^{-\tilde{j}/2}(1+2\pi\ell)) \leq 2^{-j/2}(-1-k) \quad \text{or} \quad \tan(2^{-\tilde{j}/2}(-1+2\pi\ell)) \geq 2^{-j/2}(1-k).$$

Continuing (7), this implies

$$|\langle \sigma_{j,k,m,1}, \gamma_{\tilde{j},\ell,\tilde{m}} \rangle| \leq C_{j,k,m,\tilde{j},\ell,\tilde{m}} 1_{\{k \in K_{j,\tilde{j},\ell}\}} 1_{\{\ell \in L_{j,\tilde{j},k}\}}, \quad (9)$$

with $K_{j,\tilde{j},\ell}$ and $L_{j,\tilde{j},k}$ as defined in the statement of the lemma.

Next we aim to estimate the decay in m and \tilde{m} by making use of Lemma 2.2. To prepare the application of this lemma, we rescale the function $f_{j,\tilde{j},k,\ell}$ in the term of the RHS of (4) according to

$$\hat{g}_{j,\tilde{j},k,\ell}(u, v) = 2^{j\frac{3}{2}} \hat{f}_{j,\tilde{j},k,\ell}(A_{2^j}(u, v)).$$

This yields a function which can be decomposed into factors in the following way:

$$\hat{g}_{j,\tilde{j},k,\ell}(u, v) = \tilde{W}_{0,j}(u, v) \tilde{W}_{1,j}(u, v) \tilde{V}_{0,j}(u, v) \tilde{V}_{1,j}(u, v).$$

All factors belong to C^∞ , and it can be checked that their derivatives are bounded independent on j (for a similar argument confirm [11, Subsec. 5.2]). This allows us to apply Lemma 2.2 to obtain

$$|f_{j,\tilde{j},k,\ell}(b)| \leq c_N \langle |A_{2^j} b| \rangle^{-N}, \quad N = 2, 4, 6, \dots$$

From this we conclude that, for $N = 2, 4, 6, \dots$,

$$\begin{aligned} |\langle \sigma_{j,k,m,1}, \gamma_{\tilde{j},\ell,\tilde{m}} \rangle| &= |f_{j,\tilde{j},k,\ell}(S_k^T A_{2^{-j}} m - R_{\theta_{\tilde{j},\ell}} A_{2^{-\tilde{j}}} \tilde{m})| \\ &\leq c_N \langle |A_{2^j}(S_k^T A_{2^{-j}} m - R_{\theta_{\tilde{j},\ell}} A_{2^{-\tilde{j}}} \tilde{m})| \rangle^{-N}. \end{aligned}$$

Combining this estimate with the estimates from (7) and (9) proves the lemma. \square

2.2 Proof of Theorem 1.1

Let $0 < p \leq 1$. We start by proving that

$$\sup_{\mu} \sum_{\eta} |(\langle \sigma_{\eta}, \gamma_{\mu} \rangle)_{\eta,\mu}|^p < \infty. \quad (10)$$

Setting $\eta = (j, k, m, 1)$ and $\mu = (\tilde{j}, \ell, \tilde{m})$, by Proposition 2.1,

$$\begin{aligned} \sup_{\mu} \sum_{\eta} |(\langle \sigma_{\eta}, \gamma_{\mu} \rangle)_{\eta,\mu}|^p &\leq C_{N,p} \sup_{\tilde{j},\ell,\tilde{m}} \sum_{\{|j-\tilde{j}| \leq 2\}} \sum_{\{k \in K_{j,\tilde{j},\ell}\}} \sum_m \langle |b_{j,k,m,\tilde{j},\ell,\tilde{m}}| \rangle^{-pN} \\ &\leq C'_{N,p} \sup_{\tilde{j},\ell,\tilde{m}} \sum_{\{k \in K_{j,\tilde{j},\ell}\}} \sum_m \langle |b_{j,k,m,j,\ell,\tilde{m}}| \rangle^{-pN}. \end{aligned} \quad (11)$$

The last estimate was derived by observing that the maximum of $\sum_m \langle |b_{j,k,m,j,\ell,\tilde{m}}| \rangle^{-pN}$ is attained if $\tilde{j} = j$.

We next compute the number of integers k satisfying $|k| \leq \lceil 2^{j/2} \rceil$ which are contained in $K_{j,j,\ell}$. We observe that $\#(K_{j,j,\ell})$ is maximal if ℓ is chosen so that the upper bound of the curvelet coincides with the angle bisector, the reason being that the support in frequency domain of this ‘corner curvelet’ has a maximal number of intersections with frequency supports of shearlets. In fact, the angular support of the Fourier Transform of shearlets become smaller when the angle increases, hence more shearlets are needed to overlap the angular frequency support of a curvelet, which does not change its size with varying angle (also compare the proof of Proposition 2.1). Hence, using

$$\text{supp } \hat{\gamma}_{\tilde{j},\ell,\tilde{m}} = \{(\xi_1, \xi_2) \in \mathbb{R}^2 : r \in [2^{\tilde{j}-1}, 2^{\tilde{j}+1}], \omega \in 2^{-\tilde{j}/2}[-1, 1] + \theta_{\tilde{j},\ell}\}$$

(cf. (6)), it is sufficient to restrict to the situation

$$\frac{\pi}{4} = 2^{-j/2} + \theta_{j,\ell}.$$

By definition of $\theta_{j,\ell}$, we therefore obtain the condition

$$\ell = (2\pi)^{-1}(2^{j/2}\pi/4 - 1).$$

The definition of $K_{j,j,\ell}$ implies

$$\begin{aligned} \#(K_{j,j,\ell}) &\leq -2^{j/2} \tan(2^{-j/2}(-1 + 2^{j/2}\pi/4 - 1)) - (-2^{j/2} \tan(2^{-j/2}(1 + 2^{j/2}\pi/4 - 1))) + 3 \\ &\leq 2^{j/2}(1 - \tan(\pi/4 - 2 \cdot 2^{-j/2})) + 3. \end{aligned}$$

Now

$$2^{j/2}(1 - \tan(\pi/4 - 2 \cdot 2^{-j/2})) \rightarrow 4, \quad j \rightarrow \infty,$$

hence,

$$\#(K_{j,j,\ell}) \rightarrow 7, \quad j \rightarrow \infty.$$

From (11), we can then conclude that

$$\sup_{\mu} \sum_{\eta} |(\langle \sigma_{\eta}, \gamma_{\mu} \rangle)_{\eta,\mu}|^p \leq C''_{N,p} \sup_{j,k,\ell,\tilde{m}} \sum_m \langle |b_{j,k,m,j,\ell,\tilde{m}}| \rangle^{-pN}. \quad (12)$$

Next we aim to prove that

$$\sum_m \langle |b_{j,k,m,j,\ell,\tilde{m}}| \rangle^{-pN} \leq C_{N,p} \sum_m \langle |m| \rangle^{-pN} \leq C'_{N,p}. \quad (13)$$

The second inequality follows easily from the facts that $\langle |m| \rangle^{-1} \leq 2^{-1} \langle m_1 \rangle^{-1} \langle m_2 \rangle^{-1}$ and choosing pN large enough such that $\sum_{m_i} \langle m_i \rangle^{-pN} < \infty$ for $i = 1, 2$. Concerning the first inequality in (13), recall that

$$b_{j,k,m,j,\ell,\tilde{m}} = A_{2^j}(S_k^T A_{2^{-j}} m - R_{\theta_{j,\ell}} A_{2^{-j}} \tilde{m}).$$

Since we sum over m , WLOG we can assume that $\tilde{m} = 0$. We have

$$|A_{2^j} S_k^T A_{2^{-j}} m| = |(m_1, 2^{-j/2} k m_1 + m_2)|,$$

and hence it follows immediately that

$$\sum_m \langle |A_{2^j} S_k^T A_{2^{-j}} m| \rangle^{-pN} \leq C_{N,p} \sum_m \langle |m| \rangle^{-pN}.$$

This completes the proof of (13).

Finally, (10) follows from the application of (13) to (12) and an estimate similar to Proposition 2.1 for the second cone $\mathcal{C}^{(2)}$ to handle the indices $\eta = (j, k, m, 2)$.

It remains to prove that

$$\sup_{\eta} \sum_{\mu} |(\langle \sigma_{\eta}, \gamma_{\mu} \rangle)_{\eta, \mu}|^p < \infty. \quad (14)$$

Again, by Proposition 2.1,

$$\begin{aligned} \sup_{\eta} \sum_{\mu} |(\langle \sigma_{\eta}, \gamma_{\mu} \rangle)_{\eta, \mu}|^p &\leq C_N^p \sup_{j,k,m} \sum_{\{|j-\tilde{j}|\leq 2\}} \sum_{\{\ell \in L_{j,\tilde{j},k}\}} \sum_{\tilde{m}} \langle |b_{j,k,m,\tilde{j},\ell,\tilde{m}}| \rangle^{-pN} \\ &\leq C'_N \sup_{j,k,m} \sum_{\{\ell \in L_{j,\tilde{j},k}\}} \sum_{\tilde{m}} \langle |b_{j,k,m,j,\ell,\tilde{m}}| \rangle^{-pN}. \end{aligned} \quad (15)$$

We now need to estimate $\#(L_{j,j,k})$. Recalling our ‘worst-case-discussion’ in the previous case, the number of elements in $L_{j,j,k}$ reaches its maximum if $k = 0$, i.e., the Fourier transform of the shearlet associated with k ‘sits’ precisely on the x -axis. In this case, using the definition of $L_{j,j,k}$,

$$\begin{aligned} \#(L_{j,j,k}) &\leq (2\pi)^{-1}(2^{j/2} \arctan(2^{-j/2}) - 1) - (2\pi)^{-1}(2^{j/2} \arctan(-2^{-j/2}) + 1) + 3 \\ &= (2\pi)^{-1}2^{j/2}(\arctan(2^{-j/2}) - \arctan(-2^{-j/2})) - \pi^{-1} + 3 \\ &\leq \pi^{-1}(2^{j/2} \arctan(2^{-j/2}) - 1) + 3. \end{aligned}$$

Consequently,

$$\#(L_{j,j,k}) \rightarrow 3, \quad j \rightarrow \infty.$$

Hence, continuing the computation in (15),

$$\sup_{\eta} \sum_{\mu} |(\langle \sigma_{\eta}, \gamma_{\mu} \rangle)_{\eta, \mu}|^p \leq C''_N \sup_{j,\ell,k,m} \sum_{\tilde{m}} \langle |b_{j,k,m,j,\ell,\tilde{m}}| \rangle^{-pN}.$$

Combining this estimate with

$$\sum_{\tilde{m}} \langle |b_{j,k,m,j,\ell,\tilde{m}}| \rangle^{-pN} \leq C_{N,p} \sum_{\tilde{m}} \langle |\tilde{m}| \rangle^{-pN} \leq C'_{N,p},$$

which can be proven similarly as (13) (cf. also [11, Sect. 5.2]), the claim (14) follows. This completes the proof.

3 Impact of Sparsity Equivalence

To illustrate the impact of the concept of sparsity equivalence focussing on the chosen exemplary case of curvelets and shearlets, we now discuss two different situations in which the application of Theorem 1.2 automatically leads to novel results.

We might have also included the search for optimally sparse expansions of Fourier Integral Operators of order 0. Since such a result is however already known for curvelets and shearlets – with not surprisingly quite similar proofs –, our considerations cannot lead to new results. They however point to a simplified analysis once the result was known for either curvelets or shearlets.

3.1 Optimal Sparse Representation of C^2 -Curvilinear Singularities

To efficiently process image data, optimally sparse approximations are crucial. As already discussed in Subsection 1.1, the ability to sparsely approximate a class of signals is measured by the decay of the error of the n -term approximation using the largest n coefficients in magnitude; see (1). Choosing the ‘correct’ model class for images is certainly a highly delicate task. In 2004, Candès and Donoho proposed a so-called cartoon model [9] motivated by the fact that edges are the most prominent features in images, a fact also evidenced in computer vision.

The cartoon model they proclaimed is defined as follow: Let $B \subset [0, 1]^2$ be bounded by a closed C^2 curve whose curvature is uniformly bounded by some $\nu > 0$, and let $STAR^2(\nu)$ be the class of translates of such sets B . Then the class of *cartoon-like images* $\mathcal{E}^2(\nu)$ is defined to be the set of functions f on \mathbb{R}^2 of the form

$$f = f_0 + f_1 \chi_B,$$

where $f_0, f_1 \in C^2(\mathbb{R}^2)$ with compact support in $[0, 1]^2$, $B \in STAR^2(\nu)$, and $\|f\|_{C^2} = \sum_{|\alpha| \leq 2} \|D^\alpha f\|_\infty \leq 1$.

By information theoretic arguments, it can be shown that the optimally achievable rate of sparse approximations under weak conditions on the dictionary and the selection process is N^{-2} as $N \rightarrow \infty$. For first generation curvelets [9] as well as for shearlets [16] (see also [22]), this rate is achieved up to a multiplicative log factor of $(\log N)^3$.

We now claim that also (second generation) curvelets achieve the optimal sparse approximation rate up to a factor negligible compared to N^{-2} .

Theorem 3.1 *The curvelet frame $(\gamma_\mu)_\mu$ provides (almost) optimally sparse approximations of functions $f \in \mathcal{E}^2(\nu)$, i.e., there exists some $C > 0$ such that*

$$\|f - f_N\|_2^2 \leq C \cdot N^{-2} \cdot D(N) \quad \text{as } N \rightarrow \infty,$$

where f_N is the nonlinear N -term approximation obtained by choosing the N largest curvelet coefficients of $f \in \mathcal{E}^2(\nu)$ and $N^{-\varepsilon} \cdot D(N) \rightarrow 0$ as $N \rightarrow \infty$ for all $\varepsilon > 0$.

Proof. Given some $f \in \mathcal{E}^2(\nu)$, similar to (2), it suffices to prove that

$$\sum_{n \geq N} |(\langle f, \gamma_\mu \rangle)_{(n)}|^2 \leq C \cdot N^{-2} \cdot D(N) \quad \text{as } N \rightarrow \infty \quad (16)$$

with $N^{-\varepsilon} \cdot D(N) \rightarrow 0$ as $N \rightarrow 0$ for all $\varepsilon > 0$. We remark that in the following the constants might change, by abuse of notation, we however always coin them C .

First recall that, by [16, Thm 1.1], the shearlet frame $(\sigma_\eta)_\eta$ achieves the rate

$$\sup_{g \in \mathcal{E}^2(\nu)} |(\langle g, \sigma_\eta \rangle)_{(n)}| \leq C \cdot n^{-3/2} \cdot (\log n)^{3/2} \quad \text{for each } n. \quad (17)$$

Now let $\varepsilon > 0$, and choose $p = 2/3 + \varepsilon$. Then, by (17),

$$\sup_{g \in \mathcal{E}^2(\nu)} \|(\langle g, \sigma_\eta \rangle)_\eta\|_p^p \leq \sup_{g \in \mathcal{E}^2(\nu)} C \cdot \sum_n (n^{-3/2} \cdot (\log n)^{3/2})^{2/3+\varepsilon} \leq C.$$

By Theorem 1.2, this implies that $\sup_{g \in \mathcal{E}^2(\nu)} \|(\langle g, \gamma_\mu \rangle)_\mu\|_p \leq C$. Hence, for each n ,

$$\sup_{g \in \mathcal{E}^2(\nu)} |(\langle g, \gamma_\mu \rangle)_{(n)}| \leq C \cdot n^{-1/p},$$

and therefore

$$\sum_{n \geq N} |(\langle f, \gamma_\mu \rangle)_{(n)}|^2 \leq C \cdot N^{-2/p+1} = C \cdot N^{-2} \cdot N^{\frac{9\varepsilon}{2+3\varepsilon}}.$$

In the definition of p the variable ε can be chosen arbitrarily small, which implies (16), and the theorem is proved. \square

3.2 Geometric Separation

Natural images are typically composed of morphologically distinct features; an example being spines (pointlike structures) and dendrites (curvelike structures) in neurobiological imaging. One goal is to automatically extract those components for separate analysis. In [14], the author, joint with Donoho, studied the situation of images composed of point- and curvelike structures, for which they introduced models by

$$\mathcal{P} = \sum_{i=1}^P |x - x_i|^{-3/2} \quad \text{and} \quad \mathcal{C} = \int \delta_{\tau(t)} dt, \quad \text{with } \tau : [0, 1] \mapsto \mathbb{R}^2 \text{ a closed curve,} \quad (18)$$

respectively. The *Geometric Separation Problem* now consists in extracting \mathcal{P} and \mathcal{C} from knowledge of f given by

$$f = \mathcal{P} + \mathcal{C}.$$

In [14], a particular decomposition technique based on ℓ_1 minimization was employed which required suitably chosen overcomplete systems which sparsify the different components. Using the tight frame of radial wavelets for the pointlike structures and the tight frame of curvelets for the curvelike structures, asymptotically arbitrarily precise separation was proven.

Using the results on sparsity equivalence derived in this paper, we can now prove that a different pair of representation systems can be utilized for this Geometric Separation Problem, which is more suitable for a digital realization: orthonormal separable Meyer wavelets and shearlets. In contrast to the pair considered before, surprisingly, now one system even forms an orthonormal basis.

For the reader's convenience, we first briefly recall the definition of orthonormal separable Meyer wavelets. Let $W \in L^2(\mathbb{R})$ denote the Fourier transform of the Meyer wavelet and $\phi \in L^2(\mathbb{R})$ the associated scaling function. Letting $W^h \in L^2(\mathbb{R}^2)$, $h = 1, 2, 3$ be defined by

$$W^1(\xi) = \hat{\phi}(\xi_1)W(\xi_2), \quad W^2(\xi) = W(\xi_1)\hat{\phi}(\xi_2) \quad \text{and} \quad W^3(\xi) = W(\xi_1)W(\xi_2),$$

the orthonormal separable Meyer wavelets at scale j and spatial position n are defined by their Fourier transforms

$$\hat{\psi}_\nu(\xi) = 2^{-j}W^h(\xi/2^j)e^{i\langle n, \xi \rangle/2^j},$$

where $\nu = (h, j, n)$ index type of mother function, scale, and position. This system forms an orthonormal basis for $L^2(\mathbb{R}^2)$. For each j , the functions $\hat{\psi}_\nu$ are supported on the corona $\mathcal{Z}_{2^{j+1}\pi/3}$, where

$$\mathcal{Z}_r = \{\xi \in \mathbb{R}^2 : r \leq \|\xi\|_\infty \leq 4 \cdot r\}$$

(see Figure 4). For more details we refer to [24].

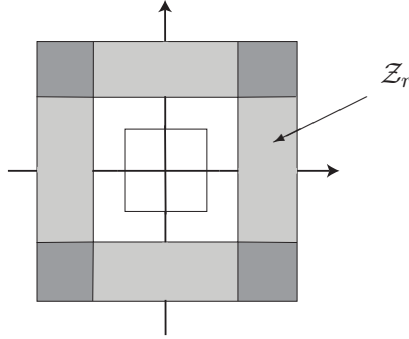


Figure 4: The tiling of the frequency domain induced by orthonormal separable Meyer wavelets.

Shearlets $\{\sigma_\eta\}_\eta$, where $\eta = (j, k, m, \iota)$ indexes scale, orientation, position, and cone, were already defined in Subsection 1.2.2, but to match them with Meyer wavelets, we now choose W to be the Fourier transform of the Meyer wavelet. We wish to draw the reader's attention to the fact that the supports of orthonormal separable Meyer wavelets match perfectly with the supports of shearlets. In fact, for each scale j , the Fourier transforms of the elements of both systems are supported on $\mathcal{Z}_{2^{j+1}\pi/3}$.

We next construct a family of filters F_j with transfer functions

$$\hat{F}_j(\xi) = W(\|\xi\|_\infty/2^j), \quad \xi \in \mathbb{R}^2$$

leading to a decomposition of a function g into functions $g_j = F_j \star f$ defined on the frequency corona $\mathcal{Z}_{2^{j+1}\pi/3}$ equipped with the reconstruction formula $g = \sum_j F_j \star g_j$. Let \mathcal{F}_j denote the range of the operator of convolution with F_j . Then shearlets at level j' are orthogonal to \mathcal{F}_j unless $|j' - j| \leq 1$. Similarly, orthonormal separable Meyer wavelets at level j' are orthogonal to \mathcal{F}_j unless $|j' - j| \leq 1$. The proofs of these two claims use precisely the same arguments as the corresponding result in [14], wherefore we omit them.

We can now formulate the corresponding Component Separation Problem (CSEP). For the sake of brevity, we let Θ_j denote the indices $\nu = (h, j, n)$ of orthonormal separable Meyer wavelets at level j , and let $\Theta_j^\pm = \Theta_{j-1} \cup \Theta_j \cup \Theta_{j+1}$. Likewise, we let Σ_j denote the indices $\eta = (j, k, m, \iota)$ of shearlets at level j , and let $\Sigma_j^\pm = \Sigma_{j-1} \cup \Sigma_j \cup \Sigma_{j+1}$. Further, we denote the filtered composed image f and the filtered point and curvilinear part \mathcal{P} and \mathcal{C} (cf. (18)) by

$$f_j = F_j \star f = F_j \star (\mathcal{P} + \mathcal{C}) = \mathcal{P}_j + \mathcal{C}_j.$$

Then we can formulate the Component Separation Problem as the following ℓ_1 minimization problem:

$$(\text{CSEP}) \quad (W_j, S_j) = \operatorname{argmin} \|(\langle W_j, \psi_\nu \rangle)_\nu\|_1 + \|(\langle S_j, \sigma_\eta \rangle)_\eta\|_1 \quad \text{subject to } f_j = W_j + S_j.$$

We claim that the considered pair of representation systems leads to asymptotically perfect separation in the sense of the following theorem. Before stating the result, we wish to remark that the proof draws from various definitions and lemmata from [14], wherefore we decided that for the sake of brevity – this being mostly an application of our main result in this paper – we only present the road map of its proof.

Theorem 3.2 *Let (W_j, S_j) denote the solution of (CSEP). Then, we have*

$$\frac{\|W_j - \mathcal{P}_j\|_2 + \|S_j - \mathcal{C}_j\|_2}{\|\mathcal{P}_j\|_2 + \|\mathcal{C}_j\|_2} \rightarrow 0, \quad j \rightarrow \infty$$

Proof. The proof presented in [14] uses as one main idea the following estimate for each scale j : Let $\mathcal{S}_{1,j}$ and $\mathcal{S}_{2,j}$ be sets of ‘significant coefficients’ of wavelets and curvelets, respectively, let δ_j be the sparse approximation error given by

$$\sum_{\nu \in \mathcal{S}_{1,j}^c} |\langle W_j, \psi_\nu \rangle| + \sum_{\eta \in \mathcal{S}_{2,j}^c} |\langle S_j, \sigma_\eta \rangle| \leq \delta_j,$$

and let $(\mu_c)_j$ be the cluster coherence defined as

$$(\mu_c)_j = \max \left\{ \max_{\eta} \sum_{\nu \in \mathcal{S}_{1,j}} |\langle \psi_\nu, \sigma_\eta \rangle|, \max_{\nu} \sum_{\eta \in \mathcal{S}_{2,j}} |\langle \psi_\nu, \sigma_\eta \rangle| \right\}.$$

Then [14, Prop. 2.1] applied to each filtered f_j implies

$$\|W_j - \mathcal{P}_j\|_2 + \|S_j - \mathcal{C}_j\|_2 \leq \frac{2\delta_j}{1 - 2(\mu_c)_j}.$$

Thus, the key step in [14] was the construction of clusters $\mathcal{S}_{1,j}$ and $\mathcal{S}_{2,j}$ having *both* of the following two properties: (i) asymptotically negligible cluster coherences:

$$(\mu_c)_j \rightarrow 0, \quad j \rightarrow \infty,$$

and (ii) asymptotically negligible cluster approximation errors:

$$\delta_j = o(\|\mathcal{P}_j\|_2 + \|\mathcal{C}_j\|_2), \quad j \rightarrow \infty.$$

The same steps with very similar argumentations can be performed for the pair wavelets-shearlets if adapted clusters $\mathcal{S}_{1,j}$ and $\mathcal{S}_{2,j}$ are defined by applying the following two key observations:

- It was shown in Theorem 1.2 that shearlets and curvelets are sparsity equivalent; more precisely, there exists a sparse matrix N_1 , say, which satisfies

$$(\langle \sigma_\eta, g \rangle)_\eta = N_1(\langle \gamma_\mu, g \rangle)_\mu$$

for any distribution g .

- Orthonormal separable Meyer wavelets and radial wavelets are likewise sparsity equivalent, i.e., there exists a sparse matrix N_2 , say, which satisfies

$$(\langle \psi_\nu, g \rangle)_\nu = N_2(\langle \psi_\lambda, g \rangle)_\lambda$$

for any distribution g .

A second ingredient are estimates for inner products between wavelets and shearlets within the frames, but also across. For this, the paralleling lemma to [14, Lem. 3.3] – with a very similar proof – is essential:

Lemma 3.1 *For each $N = 1, 2, \dots$ there is a constant c_N so that*

$$|\langle \psi_\nu, \psi_\lambda \rangle| \leq c_N \cdot 1_{\{|j-j'| < 2\}} \cdot \langle |n - n'| \rangle^{-N}, \quad \forall \nu = (h, j, n) \forall \lambda = (h', j', n').$$

As already remarked before, we will not lay out the precise details of the complete proof, since the arguments in the very lengthy and technical proof from [14] just need to be adapted in a straightforward manner to the sets of significant coefficients now based on the choice for orthonormal wavelets and shearlets. We then derive Theorem 3.2, thus perfect separation using orthonormal separable Meyer wavelets and shearlets. \square

4 Extensions and General Viewpoint

So far we focused entirely on a very special situation showing sparsity equivalence between curvelets and shearlets. Our goal was to show that for this exemplary situation sparsity equivalence can be established, provides insight into the relation between these systems, and lead automatically to novel results on sparse expansions of those two anisotropic systems.

This is however just the ‘tip of the iceberg’: the main results in this paper are susceptible of very extensive generalizations and extensions.

- *Curvelets and Shearlets.* It is conceivable that a similar statement as Theorem 1.2 is provable for first generation curvelets as also for the new class of compactly supported shearlets. It should though be mentioned that the compactly supported shearlet frames introduced so far are not tight frames, hence the framework developed in this paper needs to be extended to pairs of general frames.
- *Other Systems.* The analysis of sparsity equivalence of curvelets and shearlets we drove here can and should be applied to other pairs of systems. Ideally, novelly introduced systems could be compared to a system whose sparse approximation properties are already very well understood.

- *Systems with Continuous Parameters.* Certainly, we can also ask about similar sparsity properties for systems with continuous parameters. This however requires a different sparsity model, where one conceivable path would be to compare resolution of wavefront set behavior in the sense of [10, 20].
- *Weighted Norms.* When aiming at transferring results such as sparse decompositions of curvilinear integrals [7] or sparse decompositions of the Radon transform [8], the framework needs to be generalized to weighted ℓ_p norms. Also the analysis of associated approximation spaces requires this extension, since, for instance, the norm associated with the curvelet spaces introduced in [3, p. 67] is precisely a weighted mixed $\ell_{p,q}$ norm of the coefficient sequence.

References

- [1] J. P. Antoine, R. Murenzi, and P. Vandergheynst, *Directional wavelets revisited: Cauchy wavelets and symmetry detection in patterns*, Appl. Comput. Harmon. Anal. **6** (1999), 314–345.
- [2] R. H. Bamberger and M. J. T. Smith, *A filter bank for directional decomposition of images: theory and design*, IEEE Trans. Signal Process. **40** (1992), 882–893.
- [3] L. Borup and M. Nielsen, *Frame Decomposition of Decomposition Spaces*, J. Fourier Anal. Appl. **13** (2007), 39–70.
- [4] A. M. Bruckstein, D. L. Donoho, and M. Elad, *From Sparse Solutions of Systems of Equations to Sparse Modeling of Signals and Images*, SIAM Review **51** (2009), 34–81.
- [5] E. J. Candès, and L. Demanet, *The curvelet representation of wave propagators is optimally sparse*, Comm. Pure Appl. Math. **58** (2005), 1472–1528.
- [6] E. J. Candès and D. L. Donoho, *Ridgelets: a key to higher-dimensional intermittency?*, Phil. Trans. R. Soc. Lond. A. **357** (1999), 2495–2509.
- [7] E. J. Candès and D. L. Donoho, *Curvelets and curvilinear integrals*, J. Approx. Theory. **113** (2000), 59–90.
- [8] E. J. Candès and D. L. Donoho, *Recovering edges in ill-posed inverse problems: Optimality of curvelet frames*, Ann. Statist. **30** (2000), 784–842.
- [9] E. J. Candès and D. L. Donoho, *New tight frames of curvelets and optimal representations of objects with C^2 singularities*, Comm. Pure Appl. Math. **56** (2004), 219–266.
- [10] E. J. Candès and D. L. Donoho, *Continuous curvelet transform: I. Resolution of the wavefront set*, Appl. Comput. Harmon. Anal. **19** (2005), 162–197.
- [11] E. J. Candès and D. L. Donoho, *Continuous curvelet transform: II. Discretization of frames*, Appl. Comput. Harmon. Anal. **19** (2005), 198–222.

- [12] M. N. Do and M. Vetterli, *The contourlet transform: an efficient directional multiresolution image representation*, IEEE Trans. Image Proc. **14** (2005), 2091–2106.
- [13] D. L. Donoho, *Wedgelets: nearly minimax estimation of edges*, Ann. Statist. **27** (1999), 859–897.
- [14] D. L. Donoho and G. Kutyniok, *Microlocal Analysis of the Geometric Separation Problem*, preprint.
- [15] K. Guo, G. Kutyniok, and D. Labate, *Sparse multidimensional representations using anisotropic dilation and shear operators*, in: Wavelets and Splines, G. Chen and M. Lai (eds.), Nashboro Press, Nashville, TN (2006), 189–201.
- [16] K. Guo and D. Labate, *Optimally sparse multidimensional representation using shearlets*, SIAM J. Math. Anal. **39** (2007), 298–318.
- [17] N. Kingsbury, *Complex wavelets for shift invariant analysis and filtering of signals*, Appl. Computat. Harmon. Anal. **10** (2001), 234–253.
- [18] P. Kittipoom, G. Kutyniok, and W.-Q Lim, *Construction of Compactly Supported Shearlets*, preprint.
- [19] P. Kittipoom, G. Kutyniok, and W.-Q Lim, *Irregular Shearlet Frames: Geometry and Approximation Properties*, J. Fourier Anal. Appl., to appear.
- [20] G. Kutyniok and D. Labate, *Resolution of the Wavefront Set using Continuous Shearlets*, Trans. Amer. Math. Soc. **361** (2009), 2719–2754.
- [21] G. Kutyniok, J. Lemvig, and W.-Q Lim, *Compactly Supported Shearlets*, Approximation Theory XIII (San Antonio, TX, 2010), Springer, to appear.
- [22] G. Kutyniok, and W.-Q Lim, *Compactly Supported Shearlets are Optimally Sparse*, preprint.
- [23] G. Kutyniok, M. Shahram, and D. L. Donoho, *Development of a Digital Shearlet Transform Based on Pseudo-Polar FFT*, Wavelets XIII (San Diego, CA, 2009), 74460B-1–74460B-13, SPIE Proc. **7446**, SPIE, Bellingham, WA, 2009.
- [24] S. Mallat, *A wavelet tour of signal processing*, Academic Press, Inc., San Diego, CA, 1998.
- [25] S. Mallat and E. LePennec, *Sparse Geometric Image Representation with Bandelets*, IEEE Trans. Image Proc. **14** (2005), 423–438.